This may be the author's version of a work that was submitted/accepted for publication in the following source:

https://doi.org/10.4028/www.scientific.net/AMR.891-892.3

Molecular Dynamics Investigation on Shearing between Osteopontin and Hydroxyapatite in Biological Materials

LAI Zheng Bo[1,a], YAN Cheng[1,b] and OLOYEDE Adekunle[1,c]

[1]School of Chemistry, Physics and Mechanical Engineering,

Science and Engineering Faculty,

Queensland University of Technology,

2 George Street, GPO Box 2434, Brisbane, Australia

[a]zheng.lai@student.qut.edu.au, [b]c2.yan@qut.edu.au, [c]k.oloyede@qut.edu.au

Abstract. Bone, a hard biological material, possesses a combination of high stiffness and toughness, even though the main basic building blocks of bone are simply mineral platelets and protein molecules. Bone has a very complex microstructure with at least seven hierachical levels. This unique material characteristic attracts great attention, but the deformation mechanisms in bone have not been well understood. Simulation at nano-length scale such as molecular dynamics (MD) is proven to be a powerful tool to investigate bone nanomechanics for developing new artificial biological materials. This study focuses on the ultra large and thin layer of extrafibrillar protein matrix (thickness = ~ 1 nm) located between mineralized collagen fibrils (MCF). Non-collagenous proteins such as osteopontin (OPN) can be found in this protein matrix, while MCF consists mainly of hydroxyapatite (HA) nanoplatelets (thickness = 1.5 – 4.5 nm). By using molecular dynamics method, an OPN peptide was pulled between two HA mineral platelets with water in presence. Periodic boundary condition (PBC) was applied. The results indicate that the mechanical response of OPN peptide greatly depends on the attractive electrostatics interaction between the acidic residues in OPN peptide and HA mineral surfaces. These bonds restrict the movement of OPN peptide, leading to a high energy dissipation under shear loading.

Introduction

Bone possesses interesting material properties, especially unique mechanical properties (a combination of high stiffness and toughness) [1, 2]. For developing artificial biological materials or medical implants with similar or even better mechanical properties, bone has been widely investigated to understand its deformation and failure mechanisms. One of the main challenges is that bone has a very complex microstructure, with at least seven hierarchical levels [3]. Besides, the basic building blocks of bone are very small (e.g. thickness of mineral platelet = 1.5 – 4.5 nm) [3]. Therefore, the mechanism in bone is hardly to be understood through conventional studies at macro-level. Molecular dynamics (MD) simulation has been used previously to investigate nanomechanics in biological materials as it may provide more detailed information at smaller length scale [4-6]. The study of the bone mechanics at nano-length scale is crucial for better understanding of the bone mechanical behavior.

As a biological nanocomposite, bone has an extremely large and thin area (thickness = 1 – 2 nm) of extrafibrillar protein matrix. This layer of protein matrix can be found between mineralized collagen fibrils (MCFs), and one of the main components in MCF is the tiny hydroxyapatite (HA) platelets. The extrafibrillar protein matrix is consists of non-collagenous protein (e.g. osteopontin (OPN)). Different from tropocollagen protein, OPN protein is a highly flexible and consists of a high number of acidic amino acids (AA) [7]. As the interfacial area in nanocomposite such as bone can be up to $700 m^2/nm^3$ [8], the bone mechanical behavior greatly depends on the interaction between OPN protein and HA platelet. The adsorption of OPN peptide on HA surface has been examined previously by using atomistic simulation [5, 6]. However, the desorption of OPN peptide

from HA surface was not covered in those studies. In this work, OPN peptide was pulled between two HA platelets to investigate the shearing between OPN peptide and HA surfaces.

Methodology

GROMACS [9-12] and Visual Molecular Dynamics (VMD) [13] were used for MD simulation and visualization of the results, respectively. The computational model consists of a 18-residue OPN peptide located between two flat plates of HA mineral ($Ca_{10}[PO_4]_6[OH]_2$). The sequence of OPN peptide is DDSHQSDESHHSDESDEL and 8 of the residues are acidic residues (Aspartate and Glutamate) [5]. Each HA platelet is around 2 ns thick, with {100} crystal faces at the top and bottom surfaces. The interaction of OPN peptide to the HA {100} crystal face was studied in this study, as {100} crystal surface is believed is the main crystal face developed in the HA nanoplatelet in bone [14]. The HA initial atomic coordination is based on previous experimental work (space group $P6_3/m$ and unit cell parameters of $a = b = 9.423$ Å, $c = 6.883$ Å, $\alpha = \beta = 90^0$, $\gamma = 120^0$) [15]. The gap between two HA platelets is around 1 nm. Besides the OPN peptide and two HA platelets, the empty space of periodic boundary condition (PBC) simulation box was filled with SPC water molecules [16], and some calcium and chloride ions were included to ensure the whole system has a neutral net charge.

GROMOS force field [17] was used for OPN peptide, while Hauptmann apatite model [18] was used for HA mineral. Lennard-Jones (LJ) potential term derived from Born-Mayer-Huggins (BMH) potential term in Hauptmann apatite model was implemented in this study [19]. Lorentz-Berthelot mixing rule described in Equations 1-3 were used to calculate the intermolecular potential between OPN peptide and HA mineral [20]. Particle mesh ewald (PME) [21, 22] and a time step of 2 fs were used in MD simulation.

$$V_{LJ}\left(r_{ij}\right) = 4\varepsilon_{ij}\left(\left(\frac{\sigma_{ij}}{r_{ij}}\right)^{12} - \left(\frac{\sigma_{ij}}{r_{ij}}\right)^{6}\right) \tag{1}$$

$$\sigma_{ij} = \frac{\sigma_i + \sigma_j}{2} \tag{2}$$

$$\varepsilon_{ij} = \sqrt{\varepsilon_i \varepsilon_j} \tag{3}$$

Energy minimization with steepest descent method was performed first. 100-ps NVT and 100-ps NPT were subsequently simulated to achieve a temperature of 310K and an atmospheric pressure of 1 bar. It is followed by 5-ns MD simulation to get an equilibrated peptide structure for pulling simulation. Then, the C_α atom in C-terminal residue was pulled between the HA platelets. The pulling rate and spring constant are 0.01 nm/ps and 1000 kJ/mol nm^2, respectively.

Results and Discussion

After 5-ns MD simulation, the interaction energy between the OPN peptide and two HA platelets are extracted. The average value of van der Waals interaction energy, E_{vdw} during 5-ns MD simulation (-4 kJ/mol) is found too small compared to electrostatics interaction energy, E_{elec} (-170 kJ/mol). This indicates that the interaction between OPN peptide and HA platelets is mainly governed by the electrostatics interaction, and the van der Waals interaction has a minor effect on the OPN-HA interfacial interaction. Azzopardi et al. [6] also suggested that electrostatics plays an important role for OPN peptide interacting to HA surface. Based on the OPN peptide structure after 5-ns MD simulation shown in Figure 1(a), few side chains, mainly carboxyl groups of acidic residues, are attracted to the HA surfaces. The corresponding interaction energy plotted in Figure

1(b) shows that not all the OPN residues are strongly attracted to HA platelets. These results indicate that the interaction between OPN peptide and HA platelets is mostly due to the attractive electrostatics interaction between the acidic residues in OPN peptide and HA surfaces.
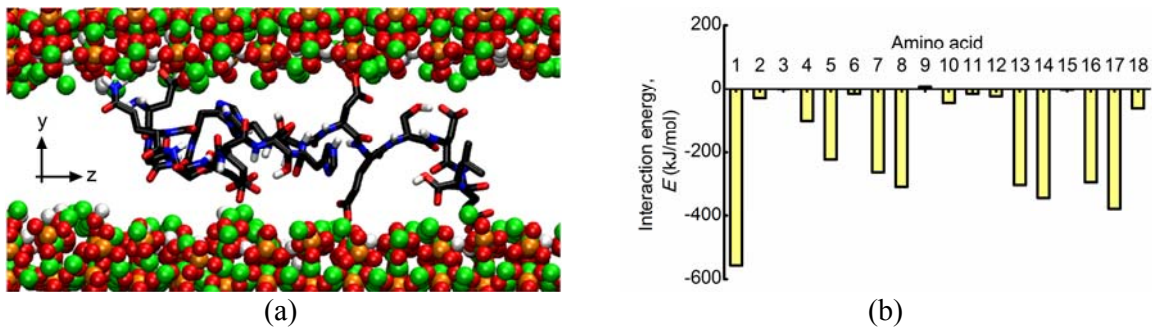

Figure 1. 5-ns MD simulation results. (a) OPN peptide structure after 5-ns MD simulation. Solvent molecules are removed for clarity. (Ca – green; P – orange; O – red; H – white; C – black; N – blue), and (b) Interaction energy between OPN residues and HA platelets after 5-ns MD simulation.

Figure 2 illustrates the OPN peptide structure during pulling simulation in positive z-direction. The pulling atom (C_α atom in C-terminal residue) is shown in purple colour. For the sake of clarity, only three acidic residues (Residues S, T, and U) are discussed and shown in colour in Figure 2. The corresponding interaction energy between these three acidic residues and HA surfaces are shown in Figure 3(a). The interaction energy is mainly contributed by electrostatics interaction energy, E_{elec}. In this work, a bond between an OPN residue and HA platelet is defined as interaction energy below -100 kJ/mol, and the OPN residues with interaction energy below -100 kJ/mol are shown in blue dotted circles in Figure 2. Based on Figure 3(a), the initial interaction energy of Residues S, T and U is below -100 kJ/mol, and these residues are close to HA surfaces as shown in Figure 2(a). However, these residues separate from HA surfaces when OPN peptide is subjected to pulling load, as observed in the OPN peptide structure during pulling simulation in Figure 2 and the interaction energy evolution in Figure 3(a). These residues subsequently reattach and detach repeatedly to HA surfaces throughout the pulling process. The simulation results also indicate that the OPN residue is able to form a new bond at different HA surface during pulling process. For instances, Residue U detaches from bottom HA surface and attaches to upper HA surface, as illustrated in Figure 2.

The initial bonds between OPN residues and HA surfaces constrain the movement of OPN peptide. Although these bonds fail while the OPN peptide is being pulled, new bonds are formed during pulling process. This explains why the measured pulling force plotted in Figure 3(b) maintains at around 2500 pN after increasing from zero. These new bonds formed during pulling process ensure the OPN peptide always sticks to HA surfaces and continuously resist the movement of OPN peptide, thus leading to high energy dissipation. As bone has an extremely large area of extrafibrillar protein matrix, the shearing between OPN peptides and HA surfaces is expected dissipating a huge amount of energy. This high energy dissipation subsequently improves the overall bone fracture resistance. This is one of the possible reasons explaining why bone has excellent fracture resistance. More studies are necessitated to further explore and understand the mechanism in bone.
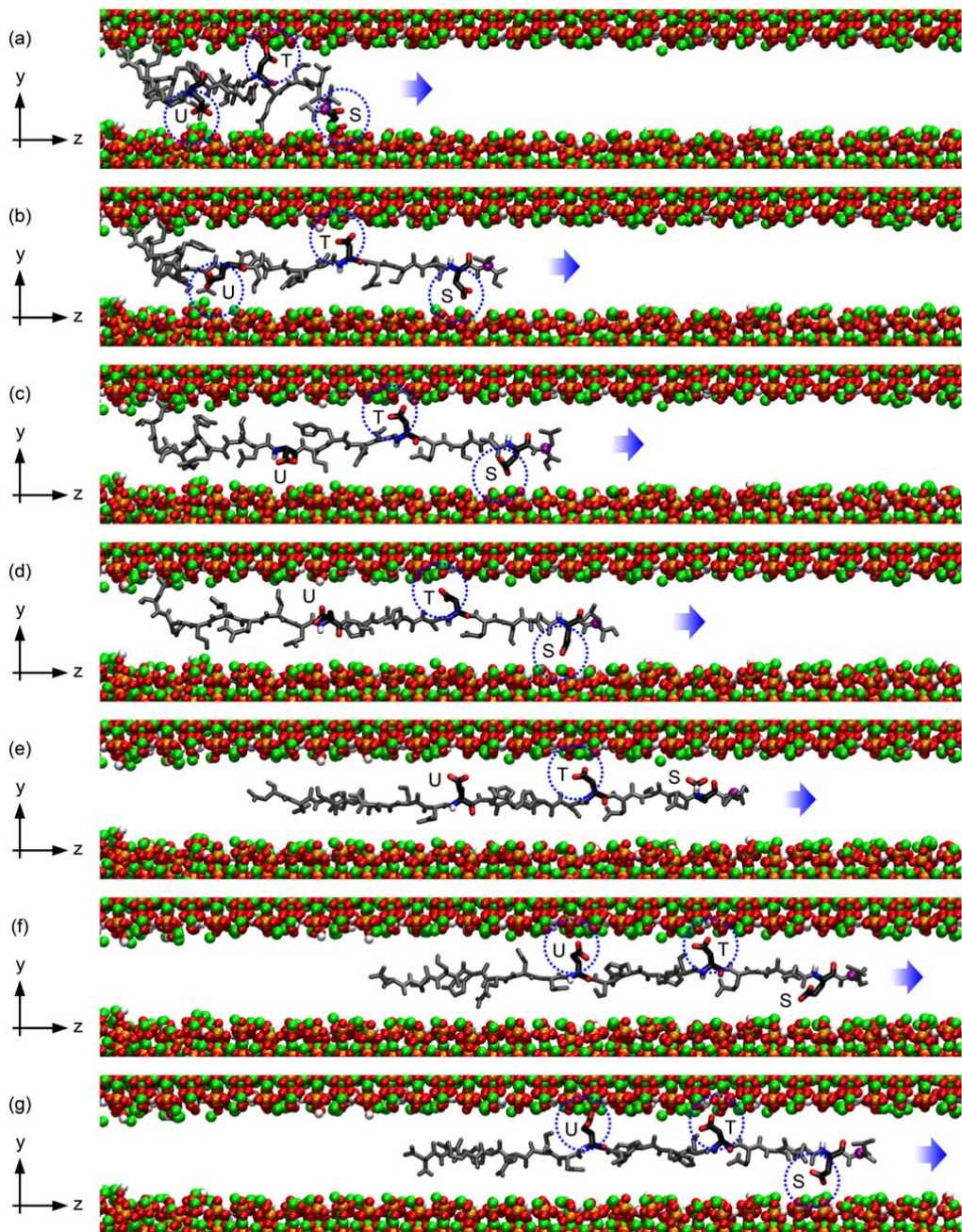
Figure 2. OPN peptide structure during pulling simulation. Solvent molecules are removed for clarity. (a) 0 nm, (b) 3.50 nm, (c) 4.50 nm, (d) 5.10 nm, (e) 7.15 nm, (f) 8.60 nm, and (g) 8.85 nm. Residues S, T, and U attracted to HA surfaces (below -100 kJ/mol) are shown in blue dotted circles. (Ca – green; P – orange; O – red; H – white; C – black; N – blue; Pulling atom (C$_\alpha$ atom) – purple).

(a)   (b)
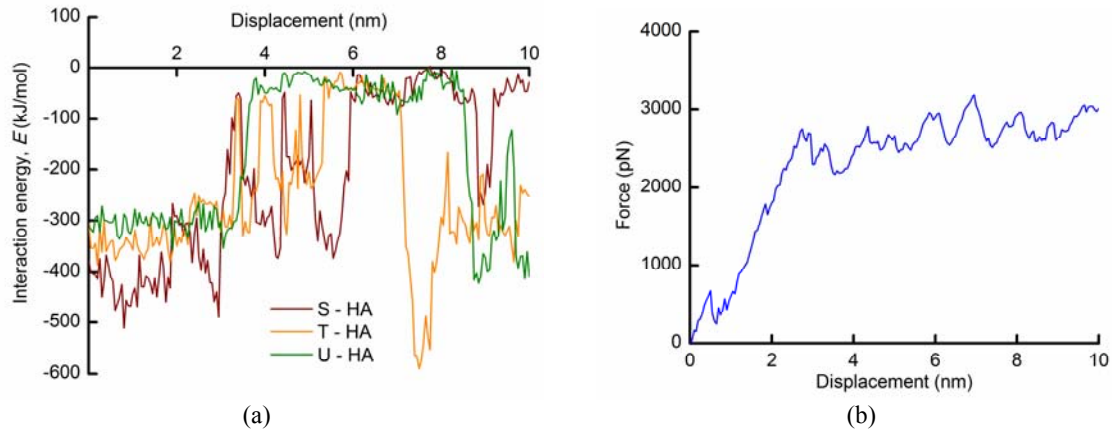
Figure 3. Pulling simulation results. (a) Interaction energy between three acidic residues (Residues S, T and U) and HA surfaces, and (b) Force-displacement curve.

Conclusions

The shearing between osteopontin (OPN) peptide and hydroxyapatite (HA) surfaces was investigated by pulling the OPN peptide between two HA platelets using molecular dynamics simulation. The results indicate that OPN-HA interfacial interaction is mainly governed by the attractive electrostatics interaction between some acidic residues of OPN peptide and HA platelets. The side chains of these acidic residues are attracted closely to the HA surfaces. These bonds fail if the OPN peptide is subjected to pulling load. However, new bonds are also formed during shearing process. These bonds continuously resist the movement of OPN peptide, and lead to high energy dissipation. As bone has a very large area of extrafibrillar protein matrix, high amount of energy is dissipated from the shearing between OPN peptides and HA surfaces. This is considered to be one of the main reasons for the excellent fracture resistance in bone.

References

[1] J.W.C. Dunlop, P. Fratzl, Biological composites, Annu. Rev. Mater. Res. 40 (2010) 1-24.
[2] U.G.K. Wegst, M.F. Ashby, The mechanical efficiency of natural materials, Philos. Mag. 84 (2004) 2167-81.
[3] M.E. Launey, M.J. Buehler, R.O. Ritchie, On the mechanistic origins of toughness in bone, Annu. Rev. Mater. Res. 40 (2010) 25-53.
[4] M.J. Buehler, S. Keten, T. Ackbarow, Theoretical and computational hierarchical nanomechanics of protein materials: Deformation and fracture, Prog. Mater. Sci. 53 (2008) 1101-241.
[5] W.N. Addison, D.L. Masica, J.J. Gray, M.D. McKee, Phosphorylation-dependent inhibition of mineralization by osteopontin ASARM peptides is regulated by PHEX cleavage, J. Bone Miner. Res. 25 (2010) 695-705.
[6] P.V. Azzopardi, J. O'Young, G. Lajoie, M. Karttunen, H.A. Goldberg, G.K. Hunter, Roles of electrostatics and conformation in protein-crystal interactions, PLoS ONE 5 (2010) 1-11.
[7] L.W. Fisher, D.A. Torchia, B. Fohr, M.F. Young, N.S. Fedarko, Flexible structures of SIBLING proteins, bone sialoprotein, and osteopontin, Biochem. Biophys. Res. Commun. 280 (2001) 460-5.
[8] R.A. Vaia, E.P. Giannelis, Polymer nanocomposites: status and opportunities, MRS Bull. 26 (2001) 391-401.

[9] H.J.C. Berendsen, D. van der Spoel, R. van Drunen, GROMACS: A message-passing parallel molecular dynamics implementation, Comput. Phys. Commun. 1995 (1995) 43-53.

[10] B. Hess, C. Kutzner, D. van der Spoel, E. Lindahl, GROMACS 4: Algorithms for highly efficient, load-balanced, and scalable molecular simulation, J. Chem. Theory Comput. 4 (2008) 435-47.

[11] E. Lindahl, B. Hess, D. van der Spoel, GROMACS 3.0: a package for molecular simulation and trajectory analysis, J. Mol. Model. 7 (2001) 306-17.

[12] D. van der Spoel, E. Lindahl, B. Hess, G. Groenhof, A.E. Mark, H.J.C. Berendsen, GROMACS: Fast, Flexible, and Free, J. Comput. Chem. 26 (2005) 1701-18.

[13] W. Humphrey, A. Dalke, K. Schulten, VMD - Visual Molecular Dynamics, J. Mol. Graph. 14 (1996) 33-8.

[14] K. Sato, T. Kogure, H. Iwai, J. Tanaka, Atomic-scale {1010} interfacial structure in hydroxyapatite determined by high-resolution transmission electron microscopy, J. Am. Ceram. Soc. 85 (2002) 3054-8.

[15] R.M. Wilson, J.C. Elliott, S.E.P. Dowker, Rietveld refinement of the crystallographic structure of human dental enamel apatites, Am. Mineral. 84 (1999) 1406-14.

[16] J. Hermans, H.J.C. Berendsen, W.F. Van Gunsteren, J.P.M. Postma, A consistent empirical potential for water-protein interactions, Biopolymers 23 (1984) 1513-8.

[17] W.F. van Gunsteren, S.R. Billeter, A.A. Eising, P.H. Hünenberger, P. Krüger, A.E. Mark, W.R.P. Scott, I.G. Tironi, Biomolecular simulation: The GROMOS96 manual and user guide, Zürich, Switzerland, 1996.

[18] S. Hauptmann, H. Dufner, J. Brickmann, S.M. Kast, R.S. Berry, Potential energy function for apatites, Phys. Chem. Chem. Phys. 5 (2003) 635-9.

[19] H. Pan, J. Tao, T. Wu, R. Tang, Molecular simulation of water behaviors on crystal faces of hydroxyapatie, Front. Mater. Sci. China 2 (2007) 156-63.

[20] J.O. Hirschfelder, C.F. Curtiss, R.B. Bird, Molecular theory of gases and liquids, New York, 1954.

[21] T. Darden, D. York, L. Pedersen, Particle mesh Ewald: An N.log(N) method for Ewald sums in large systems, J. Chem. Phys. 98 (1993) 10089-93.

[22] U. Essmann, L. Perera, M.L. Berkowitz, T. Darden, H. Lee, L.G. Pedersen, A smooth particle mesh Ewald method, J. Chem. Phys. 103 (1995) 8577-93.